

# Digital Type Disturbance Compensation Control of a Floating Underwater Robot with 2 Link Manipulator

Takashi Yatoh      Shinichi Sagara      Masakazu Tamura

Department of Control Engineering, Kyushu Institute of Technology  
Tobata, Kitakyushu 804-8550, Japan  
E-mail: sagara@cctl.kyutech.ac.jp

## Abstract

We have proposed continuous and discrete time resolved acceleration control methods for underwater vehicle-manipulator systems and the effectiveness of the control methods have been shown by experiments. In this paper, we propose a digital type disturbance compensation control method based on the RAC method considering singular configuration of manipulator. Experimental results show the effectiveness of the proposed method.

## 1 Introduction

Underwater Vehicle-Manipulator Systems (UVMSs) are expected to make important roles in ocean exploration. Many studies about dynamics and control of UVMS have been reported [1–3], however the experimental studies are only a few. We have proposed analog and digital Resolved Acceleration Control (RAC) methods for UVMS [4–7], and the effectiveness of the RAC methods are demonstrated by using a floating underwater robot with vertical planar 2-link manipulator. Furthermore, we have proposed a RAC method

considering singular configuration of manipulator [8].

In general, added mass, added moment of inertia and drag coefficient are used constant value that depends on the shape of the robots [9]. Our proposed methods described above can reduce the influence of hydrodynamic force by position and velocity feedbacks.

In this paper, to obtain higher control performance we propose a digital type disturbance compensation control method based on the RAC method considering singular configuration of manipulator. The influence of hydrodynamic force is treated as a disturbance, and the disturbance is compensated by using a disturbance observer. To verify the effectiveness of the RAC method with the disturbance observer, experiments using the 2-link underwater robot are performed. The experimental results show that the control method has a good control performance.

## 2 Modeling

The underwater robot model used in this paper is shown in Fig. 1. It has a robot base and a 2-DOF manipulator which can move in a vertical plane. Thrusters are mounted on the base to provide propulsion for position and attitude control of the base.

Symbols used in this paper are defined as follows:

- $\Sigma_U$ : inertial coordinate frame
- $\Sigma_i$ : link  $i$  coordinate frame ( $i = 0, 1, 2$ ; link 0 means base)
- ${}^U R_i$ : coordinate transformation matrix from  $\Sigma_i$  to  $\Sigma_U$
- $\mathbf{p}_e$ : position vector of end-tip of manipulator with respect to  $\Sigma_U$
- $\mathbf{p}_i$ : position vector of origin of  $\Sigma_i$  with respect to  $\Sigma_U$
- $\mathbf{v}_i$ : linear velocity vector of  $\Sigma_i$  with respect to  $\Sigma_U$
- $\boldsymbol{\omega}_i$ : angular velocity vector of  $\Sigma_i$  with respect to  $\Sigma_U$
- $\mathbf{x}_0$ : position and attitude vector of  $\Sigma_0$  with respect to  $\Sigma_U$  ( $= [\mathbf{p}_0^T, \phi_0^T]^T$ )
- $\phi_i$ : relative angle of joint  $i$

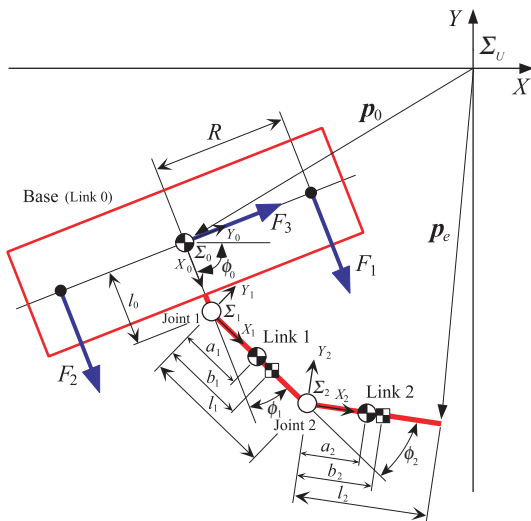


Fig. 1 2-link underwater robot model

$\phi$ : relative joint angle vector ( $= [\phi_1, \phi_2]^T$ )

$l_i$ : length of link  $i$

$\mathbf{a}_i$ : position vector from joint  $i$  to center of gravity of link  $i$  with respect to  $\Sigma_i$

$\mathbf{b}_i$ : position vector from joint  $i$  to center of buoyancy of link  $i$  with respect to  $\Sigma_i$

$F_j$ : thruster force ( $j = 1, 2, 3$ )

$R$ : length form origin of  $\Sigma_0$  to thruster

From Fig. 1 kinematic and momentum equations can be obtained [4]:

$$\dot{\mathbf{p}}_e = \mathbf{A}\dot{\mathbf{x}}_0 + \mathbf{B}\dot{\phi}, \quad \mathbf{s} = \mathbf{C}\dot{\mathbf{x}}_0 + \mathbf{D}\dot{\phi} \quad (1)$$

where  $\mathbf{A} \in R^{2 \times 3}$  and  $\mathbf{B} \in R^{2 \times 2}$  are matrices consisting of attitude angle of base and joint angles.  $\mathbf{C} \in R^{3 \times 3}$  and  $\mathbf{D} \in R^{3 \times 2}$  are matrices including the added mass  $\mathbf{M}_{a_i}$  and the added inertia  $\mathbf{I}_{a_i}$ .

In the meanwhile, the drag force and moment of joint  $i$  can be generally represented as follows [10]:

$$\mathbf{f}_{d_i} = \frac{\rho}{2} C_{D_i} D_i \int_0^{l_i} \|\mathbf{w}_i\| \mathbf{w}_i d\hat{\mathbf{x}}_i \quad (2)$$

$$\mathbf{t}_{d_i} = \frac{\rho}{2} C_{D_i} D_i \int_0^{l_i} \hat{\mathbf{x}}_i \times \|\mathbf{w}_i\| \mathbf{w}_i d\hat{\mathbf{x}}_i \quad (3)$$

where  $\mathbf{w}_i = \mathbf{v}_i + \boldsymbol{\omega}_i \times \hat{\mathbf{x}}_i$  and  $\hat{\mathbf{x}}_i = [x_i, 0, 0]^T$ ,  $\rho$  is the fluid density,  $C_{D_i}$  is the drag coefficient,  $D_i$  is the width of link  $i$ . Furthermore, the gravitational and buoyant forces acting on link  $i$  are described as follows:

$$\mathbf{f}_{g_i} = (\mathbf{R}_i)^T (\rho V_i - m_i) \mathbf{g} \quad (4)$$

$$\mathbf{t}_{g_i} = (\mathbf{R}_i)^T (\mathbf{b}_i \times \rho V_i - \mathbf{a}_i \times m_i) \mathbf{g} \quad (5)$$

where  $V_i$  and  $m_i$  are the volume and mass of link  $i$ , and  $\mathbf{g}$  is the gravitational acceleration vector.

Considering the hydrodynamic forces and using Newton-Euler formulation, the following equation of motion can be obtained:

$$\mathbf{M}(\mathbf{q})\ddot{\mathbf{q}} + \mathbf{N}(\mathbf{q}, \dot{\mathbf{q}})\dot{\mathbf{q}} + \mathbf{f}_H = [f_x \ f_y \ \tau_0 \ \tau_1 \ \tau_2]^T \quad (6)$$

where  $\mathbf{q} = [\mathbf{x}_0^T \ \phi^T]^T$  and  $\mathbf{M}(\mathbf{q})$  is the inertia matrix consisting of the added mass and inertia,  $\mathbf{N}(\mathbf{q}, \dot{\mathbf{q}})\dot{\mathbf{q}}$  is the vector of Coriolis and centrifugal forces,  $\mathbf{f}_H$  is the vector consisting of the drag and lift forces.  $f_x$  and  $f_y$  are input forces of the  $X$  and  $Y$  directions,  $\tau_i$  ( $i = 0, 1, 2$ ) is the joint torque.

With respect to the base input  $\mathbf{u}_B = [f_x \ f_y \ \tau_0]^T$  and joint input  $\mathbf{u}_M = [\tau_1 \ \tau_2]^T$ , matrices and vectors of Eq. (6) can be represented by the following block matrices:

$$\mathbf{M} = \begin{bmatrix} \mathbf{M}_{BB} & \mathbf{M}_{BM} \\ \mathbf{M}_{MB} & \mathbf{M}_{MM} \end{bmatrix}, \quad \mathbf{N} = \begin{bmatrix} \mathbf{N}_{BB} & \mathbf{N}_{BM} \\ \mathbf{N}_{MB} & \mathbf{N}_{MM} \end{bmatrix},$$

$$\mathbf{f}_H = [\mathbf{f}_{HB}^T \ \mathbf{f}_{HM}^T]^T, \quad \mathbf{u} = [\mathbf{u}_B^T \ \mathbf{u}_M^T]^T$$

Then, for a disturbance compensation described in the next section the following equation with respect to the base input can be obtained:

$$\mathbf{M}_{BB}\ddot{\mathbf{x}}_0 + \mathbf{M}_{BM}\ddot{\phi} + \mathbf{N}_{BB}\dot{\mathbf{x}}_0 + \mathbf{N}_{BM}\dot{\phi} + \mathbf{f}_{HB} = \mathbf{u}_B \quad (7)$$

### 3 Control Method

#### 3.1 Digital RAC [8]

Differentiating Eq. (1) with respect to time, the following equation can be obtained:

$$\mathbf{W}(t)\boldsymbol{\alpha}(t) = \boldsymbol{\beta}(t) + \mathbf{f}(t) - \dot{\mathbf{W}}(t)\mathbf{v}(t) \quad (8)$$

where

$$\mathbf{W} = \begin{bmatrix} \mathbf{C} + \mathbf{E} & \mathbf{D} \\ \mathbf{A} & \mathbf{B} \end{bmatrix}, \quad \boldsymbol{\alpha} = [\ddot{\mathbf{x}}_0^T \ \ddot{\phi}^T]^T,$$

$$\boldsymbol{\beta} = [\ddot{\mathbf{x}}_0^T \ \ddot{\mathbf{p}}_e^T]^T, \quad \mathbf{f} = [\dot{\mathbf{s}}^T \ \mathbf{0}^T]^T, \quad \mathbf{v} = [\dot{\mathbf{x}}_0^T \ \dot{\phi}^T]^T$$

$\dot{\mathbf{s}}$  is the external force including hydrodynamic force and thrust of the thruster which act on the base, and  $\mathbf{E}$  is the unit matrix.

Discretizing Eq. (8) by a sampling period  $T$ , and applying  $\boldsymbol{\beta}(k)$  and  $\dot{\mathbf{W}}(k)$  to the backward Euler approximation, we have

$$\mathbf{W}(k)\boldsymbol{\alpha}(k-1) = \frac{1}{T} [\boldsymbol{\nu}(k) - \boldsymbol{\nu}(k-1) + T\mathbf{f}(k) - \{\mathbf{W}(k) - \mathbf{W}(k-1)\}\mathbf{v}(k)] \quad (9)$$

where  $\boldsymbol{\nu} = [\dot{\mathbf{x}}_0^T, \dot{\mathbf{p}}_e^T]$ . Note that a computational time delay is introduced into Eq. (9).

For  $\boldsymbol{\alpha}(k)$  and  $\boldsymbol{\nu}(k)$  in Eq. (9), the desired acceleration  $\boldsymbol{\alpha}_d(k)$  and velocity  $\boldsymbol{\nu}_d(k)$  are defined as

$$\boldsymbol{\alpha}_d(k) = \frac{1}{T} \mathbf{W}^{-1}(k) [\boldsymbol{\nu}_d(k+1) - \boldsymbol{\nu}_d(k) + \boldsymbol{\Lambda} \mathbf{e}_\nu(k) + T\mathbf{f}(k)] \quad (10)$$

$$\boldsymbol{\nu}_d(k) = \frac{1}{T} \{\mathbf{p}_d(k) - \mathbf{p}_d(k-1) + \boldsymbol{\Gamma} \mathbf{e}_p(k-1)\} \quad (11)$$

where  $\boldsymbol{\Lambda} = \text{diag}\{\lambda_i\}$  and  $\boldsymbol{\Gamma} = \text{diag}\{\gamma_i\}$  ( $i = 1, \dots, 5$ ) are the velocity and position feedback gain matrices,  $\mathbf{e}_\nu(k) = \boldsymbol{\nu}_d(k) - \boldsymbol{\nu}(k)$  and  $\mathbf{e}_p(k) = \mathbf{p}_d(k) - \mathbf{p}(k)$  are the velocity and position error vectors,  $\mathbf{p}_d(k)$  is the desired value of  $\mathbf{p}(k) = [\mathbf{x}_0^T(k), \mathbf{p}_e^T(k)]^T$ . When  $\lambda_i$  and  $\gamma_i$  are selected to satisfy  $0 < \lambda_i < 1$  and  $0 < \gamma_i < 1$ ,  $\mathbf{e}_p(k) \rightarrow \mathbf{0}$  ( $k \rightarrow \infty$ ) is guaranteed.

In order to avoid the singular configuration of manipulator, the desired value of the base is modified by using the determinant of the Jacobian matrix  $J(k) = \det \mathbf{J}(k)$  of manipulator. The desired linear acceleration of the base  $\ddot{\mathbf{p}}_{0_d} = [\ddot{\mathbf{p}}_{0_{x_d}}, \ddot{\mathbf{p}}_{0_{y_d}}]$  is defined as

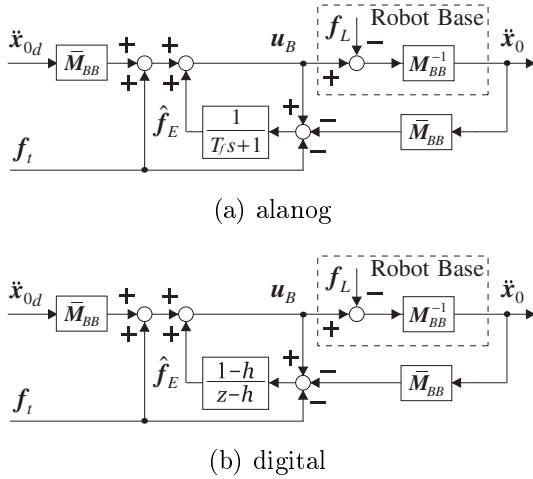


Fig. 2 Disturbance compensation

$$\ddot{p}_{0_d} = \begin{cases} \dot{p}_{e_d} & (k_1 \leq k < k_1 + n) \\ 0 & (\text{otherwise}) \\ -\dot{p}_{e_d} & (k_2 \leq k < k_2 + n) \end{cases} \quad (12)$$

where  $\dot{p}_{e_d}$  is the desired linear velocity of the end-tip of the manipulator, and  $k_1 T$  and  $k_2 T$  are the time when  $|J(k)|$  becomes less or greater than a threshold  $J_s$ , respectively, and  $nT$  is the acceleration time.

### 3.2 Disturbance compensation

In general, added mass and moment of inertia and drag coefficient are used constant value that depends on the shape of robots [9]. Our proposed methods described above can reduce the influence of hydrodynamic force by position and velocity feedbacks.

Here, to obtain higher control performance, the influence of hydrodynamic force with respect to the base is treated as a disturbance and a disturbance compensation method is introduced.

The nominal model of  $M_{BB}$  in Eq. (7) is defined as  $\bar{M}_{BB}$ . In  $\bar{M}_{BB}$  the added mass and moment of inertia and the drag coefficient are constant. Furthermore, the following force is similarly defined:

$$f_t = \bar{M}_{BM}\ddot{\phi}_d + \bar{N}_{BB}\dot{x} + \bar{N}_{BM}\dot{\phi} + \bar{f}_{HB} \quad (13)$$

where  $\bar{M}_{BM}$ ,  $\bar{N}_{BB}$ ,  $\bar{N}_{BM}$  and  $\bar{f}_{HB}$  are nominal.

When the modeling error with respect to the hydrodynamic force regards the disturbance  $f_E$ , the following estimated value can be obtained:

$$\hat{f}_E = F(s)(u_B - \bar{M}_{BB}\ddot{x}_{0_d} - f_t) \quad (14)$$

where  $F(s) = 1/(T_f s + 1)$  and  $\ddot{x}_{0_d}$  is the desired value of  $\ddot{x}_0$ ,  $T_f$  is a time constant.

Using Eqs. (13) and (14) we have the following control input of the base:

Table 1 Physical parameters of underwater robot

	Base	Link 1	Link 2
Mass [kg]	26.04	4.25	1.23
Moment of inertia [kg m <sup>2</sup> ]	1.33	0.19	0.012
Link length (x axis) [m]	0.2	0.25	0.25
Link length (y axis) [m]	0.81	0.04	0.04
Link width [m]	0.42	0.12	0.12
Added mass(x) [kg]	72.7	1.31	0.1
Added mass(y) [kg]	6.28	3.57	2.83
Added moment of inertia [kg m <sup>2</sup> ]	1.05	0.11	0.06
Drag coefficient (x)	1.2	0	0
Drag coefficient (y)	1.2	1.2	1.2

$$u_B = \bar{M}_{BB}\ddot{x}_{0_d} + f_t + \hat{f}_E \quad (15)$$

The configuration of the disturbance compensation is shown in Fig. 2(a). In Fig. 2(a)  $f_L$  is the external force of the base excepting  $\bar{M}_{BB}\ddot{x}_0$ . Furthermore, for the digital control system, Fig. 2(a) is discretized to Fig. 2(b) [11]. In Fig. 2(b)  $h = e^{-T_f/T}$ .

## 4 Experiment

In this section, to verify the effectiveness of the proposed control method, experiments are done.

Physical parameters of the underwater robot are shown in Table 1. The details of the system and the thruster characteristics are shown in the reference [8].

The experiments are carried out under the following condition. The desired end-tip position is set up along a straight path from the initial position to the target. On the other hand, the basic desired position and attitude of the base is set up the initial values, and the threshold of the determinant of the Jacobian matrix is  $J_s = 0.045$ . The sampling period is  $T=1/60$ [s], the time constant of the filter is  $T_f = 10$ [s], and the feedback gains are  $\Lambda = \text{diag}\{0.3, 0.3, 0.2, 0.2, 0.2\}$  and  $\Gamma = \text{diag}\{0.3, 0.3, 0.2, 0.2, 0.2\}$ . Furthermore, the initial relative joint angles are  $\phi_0 = -\pi/2$ [rad],  $\phi_1 = \pi/3$ [rad] and  $\phi_2 = -5\pi/18$ [rad].

The motion of the robot with the disturbance compensation is shown in Fig. 3. From Fig. 3, it can be seen that the end-tip follows the desired trajectory. The time history of the results with and without the disturbance compensation are shown in Fig. 4 and 5. From these figures, we can see that the base position and attitude errors become small values using the disturbance compensation. Furthermore, reducing the base errors the end-tip position error is also reduced. Therefore, the control performance can be improved by using the proposed method.

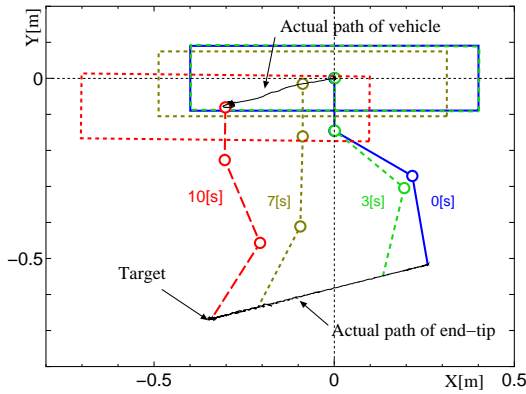


Fig. 3 Motion with disturbance compensation

## 5 Conclusion

In this paper, a digital RAC method for UVMS using disturbance compensation was proposed. The experimental results showed the effectiveness of the proposed method.

## References

- [1] T. W. McLain *et al.*, “Experiments in the Coordinated Control of an Underwater Arm/Vehicle System”, *Autonomous Robots 3*, Kluwer Academic Publishers, pp. 213 – 232, 1996.
- [2] G. Antonelli *et al.*, “Tracking Control for Underwater Vehicle-Manipulator Systems with Velocity Estimation”, *IEEE J. Oceanic Eng.*, Vol. 25, No. 3, pp. 399 – 413, 2000.
- [3] N. Sarkar, T. K. Podder, “Coordinated Motion

Planning and Control of Autonomous Underwater Vehicle-Manipulator Systems Subject to Drag Optimization”, *IEEE J. Oceanic Eng.*, Vol. 26, No. 2, pp. 228 – 239, 2001.

- [4] S. Yamada, S. Sagara, “Resolved Motion Rate Control of an Underwater Robot with Vertical Planar 2-Link Manipulator”, *Proc. AROB 7th*, pp. 230 – 233, 2002.
- [5] S. Sagara, “Digital Control of an Underwater Robot with Vertical Planar 2-Link Manipulator”, *Proc. AROB 8th*, pp. 524 – 527, 2003.
- [6] S. Sagara *et al.*, “Experiment of Digital RAC for an Underwater Robot with vertical Planar 2-Link Manipulator”, *Proc. AROB 9th*, pp. 337 – 340, 2004.
- [7] T. Yatoh *et al.*, “RAC for Underwater Vehicle-Manipulator Systems Using Dynamic Equation”, *Proc. AROB 11th*, pp. 233 – 236, 2006.
- [8] S. Sagara *et al.*, “Digital RAC for Underwater Vehicle-Manipulator Systems Considering Singular Configuration”, *J. AROB*, Vol. 10, No. 2, pp. 106 – 111, 2006.
- [9] T. I. Fossen, *Guidance and Control of Ocean Vehicles*, John Wiley & Sons, pp. 431–452, 1995.
- [10] B. Lévesque, M. J. Richard, “Dynamic Analysis of a Manipulator in a Fluid Environment”, *Int. J. Robot. Res.*, Vol. 13, No. 3, pp. 221 – 231, 1994.
- [11] I. Godler *et al.*, “Design Guidelines for Disturbance Observer’s Filter in Discrete Time”, *Proc. 7th Int. Workshop on Advanced Motion Control*, pp. 390 – 395, 2002.

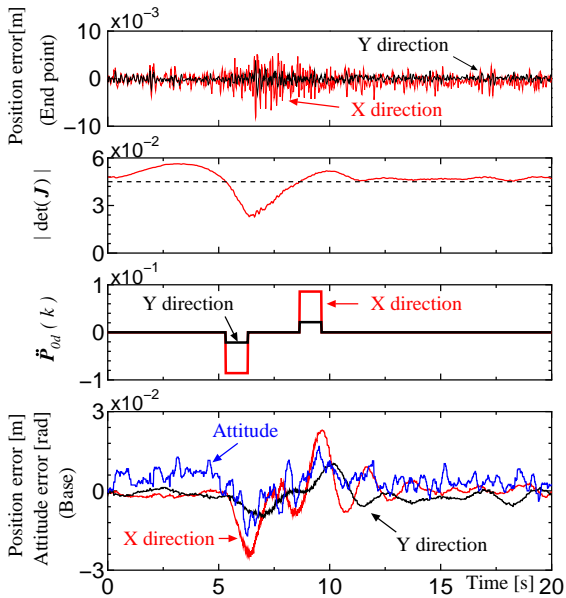


Fig. 4 Result with disturbance compensation

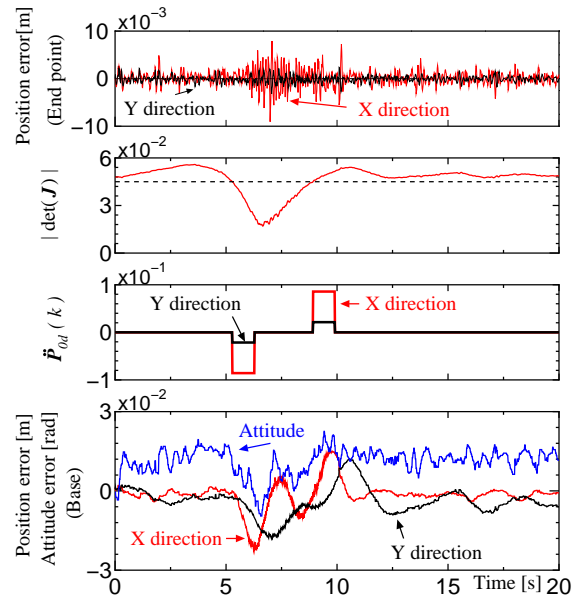


Fig. 5 Result without disturbance compensation